Chem Soc Rev

RSC Publishing

TUTORIAL REVIEW

Cosmic-ray astrochemistry

Cite this: *Chem. Soc. Rev.*, 2013, **42**, 7763

Received 1st March 2013

DOI: 10.1039/c3cs60087d

www.rsc.org/csr

Nick Indriolo*[a] and Benjamin J. McCall[b]

Gas-phase chemistry in the interstellar medium is driven by fast ion–molecule reactions. This, of course, demands a mechanism for ionization, and cosmic rays are the ideal candidate as they can operate throughout the majority of both diffuse and dense interstellar clouds. Aside from driving interstellar chemistry *via* ionization, cosmic rays also interact with the interstellar medium in ways that heat the ambient gas, produce gamma rays, and produce light element isotopes. In this paper we review the observables generated by cosmic-ray interactions with the interstellar medium, focusing primarily on the relevance to astrochemistry.

Key learning points

- Ionization of atoms and molecules by cosmic rays initiates the fast ion–molecule chemistry in the interstellar medium.
- Observed abundances of interstellar molecules are used to infer the cosmic-ray ionization rate.
- Cosmic rays provide a source of energy to the interiors of dense molecular clouds.
- Fragmentation of heavier elements by cosmic rays produces light elements such as Li, Be, and B.
- Gamma-ray observations trace the interaction of cosmic-ray protons and electrons with the interstellar medium and radiation field.

1 Introduction

The gas and dust that reside in the vast expanse of space between stars—collectively referred to as the interstellar medium (ISM)—have long been subjects of study for modern astronomy. Physical conditions in the ISM vary widely, ranging from extremely tenuous hot plasmas to self-gravitating clouds of cold gas. Different phases of the ISM and some of their general characteristics include: (i) the hot ionized medium—extremely low density ($n \approx 10^{-3}$ cm^{-3}), hot ($T \approx 10^6$ K) plasma where several atomic species are observed to be multiply ionized (*e.g.*, C^{3+}, O^{5+});† (ii) the warm ionized medium—low density ($n \approx 0.1$ cm^{-3}), warm ($T \approx 8000$ K) partially ionized gas traced by emission following electron recombination such as Hα;‡ (iii) the warm neutral medium—low density ($n \approx 0.5$ cm^{-3}), warm ($T \approx 8000$ K) neutral gas traced by 21 cm emission of hydrogen atoms due to electron spin flip; (iv) the cold neutral medium—moderate density ($n \approx 50$ cm^{-3}), cool ($T \approx 100$ K) neutral gas where hydrogen is still predominantly in atomic form, often referred to as diffuse atomic clouds; and (v) molecular clouds—moderate-to-high density, cool-to-cold neutral gas where hydrogen is predominantly in molecular form, *i.e.*, H_2. This phase is further separated into diffuse molecular clouds ($n \approx 100$ cm^{-3}, $T \approx 70$ K) that are partially transparent to ultraviolet photons, and dense molecular clouds ($n > 10^4$ cm^{-3}, $T < 30$ K) that are opaque to UV photons and are generally well-defined, self-gravitating structures. The interested reader is directed to McKee (1995),[1] Ferrière (2001)[2] and Snow and McCall (2006)[3] for more detailed information on the different ISM phases. In this review we will focus primarily on the cold neutral medium and molecular clouds, regions where collisional timescales are short enough and gas is sufficiently shielded from energetic photons such that molecular species are prevalent. Even in these regions typical terrestrial chemistry does not apply, and ionic species that on earth would rapidly react with almost anything survive long enough that observable abundances are maintained, and become important reactants in the web of interstellar chemistry.

Conditions in all of the different ISM phases are largely determined by the heating and cooling mechanisms responsible for injecting or removing energy. Cooling occurs when collisional excitation of ions, atoms, and molecules is followed by emission of a photon that escapes the parcel of gas under consideration, effectively removing kinetic energy from the system. The species that dominate radiative cooling vary

[a] *Department of Physics & Astronomy, Johns Hopkins University, 3400 N. Charles St., Baltimore, MD, 21218, USA. E-mail: indriolo@pha.jhu.edu; Fax: + 1 410-516-7239; Tel: + 1 410-516-4378*

[b] *Department of Chemistry, University of Illinois at Urbana-Champaign, 600 S. Mathews Ave., Urbana, IL, USA 61801*

† Note that astronomers often refer to the actual species using spectroscopic notation, *e.g.*, C IV for C^{3+} and O VI for O^{5+}.

‡ Hα is shorthand for the $n = 3$–2 Balmer series line in hydrogen at 656.28 nm.

depending on the gas conditions, but generally the upper state must be collisionally excitable (*i.e.*, there must be enough kinetic energy in the gas to populate the excited state), and the emited photon must be able to escape the region without being re-absorbed. Some examples include emission from fine-structure levels of C^+ at 158 μm ($^2P^0_{3/2}$–$^2P^0_{1/2}$), which dominates cooling in the cold neutral medium, and emission from rotational levels of CO and H_2O, which dominate in dense molecular clouds.

Heating, of course, is the reverse process where kinetic energy is added to the system under consideration, and there are several mechanisms for doing so in the ISM. Shock waves from supernovae and stellar winds can directly add kinetic energy to the gas. Energetic particles (cosmic rays) and photons can ionize atomic and molecular species, after which the free electron tranfers its kinetic energy to the gas *via* collisions. Energetic photons can also be absorbed by small dust grains and large molecules known as PAHs (polycyclic aromatic hydrocarbons), thought to be ubiquitous throughout the ISM. This energy goes into electrons that can diffuse throughout and potentially escape from the grain/PAH, and again collisions transfer the energy to the gas. This process, known as photoelectric heating, dominates in diffuse atomic and diffuse molecular clouds, while cosmic-ray heating becomes important in dense clouds, as will be mentioned later.

It is the balance of these heating and cooling mechanisms that determines conditions in the different ISM phases. By accounting for these processes various studies[4–6] have found that the warm ionized medium, warm neutral medium, and cold neutral medium can all exist in rough pressure equilibrium with the densities and temperatures quoted above. Molecular clouds are not in pressure equilibrium with their surroundings, but are instead self-gravitating structures, as previously mentioned. Indeed, it is the collapse of these clouds to ever higher densities that eventually results in the formation of new stars.[7–9] All of this introductory material on heating, cooling, and physics in the ISM is discussed in greater detail in several well-written textbooks, and the interested reader is referred to *The Physics and Chemistry of the Interstellar Medium* by A. G. G. M. Tielens[10] and *Astrophysics of Gaseous Nebulae and Active Galactic Nuclei* by D. E. Osterbrock and G. J. Ferland.[11]

As with physics in the ISM, interstellar chemistry can also vary widely depending on the environment. Gas-phase reactions dominate in diffuse atomic, diffuse molecular, and dense molecular clouds,[12,13] and reactions on the surfaces of dust grains increase in importance in cold, dense clouds.[14] In all of these environments, the gas phase chemistry is thought to be driven by ion–neutral reactions, which, with no activation energy barriers, typically have larger rate coefficients ($k \sim 10^{-9}$ cm^3 s^{-1}), than neutral–neutral reactions ($k \sim 10^{-11}$ cm^3 s^{-1}). Ion–neutral chemistry inherently requires some ionization mechanism, and both photons and cosmic rays are potential candidates. However, photons with $E > 13.6$ eV do not travel very far from their points of origin before being absorbed due to the prevalence of neutral, atomic hydrogen in the ISM. This means photoionization is only efficient for species with ionization potentials below that of hydrogen (*e.g.*, C, Si, Cl). For atomic hydrogen and species with higher ionization potentials—*e.g.*, He, O, N, H_2, D—there is a lack of ionizing photons in interstellar clouds. As a result, these species are primarily ionized by cosmic rays, which can operate through the entirety of the molecular ISM.

2 Cosmic-ray history and basics

In the early twentieth century, a background signal seen with electroscopes was attributed to some source of highly penetrating radiation. It was hypothesized that this radiation was due to the decay of radioactive nuclei in the earth and the atmosphere, a scenario that predicts the background signal decreasing with increased altitude. In 1912 Victor Hess discovered *via* balloon-born electroscopes that the rate of ionizing radiation *increased* at higher altitudes to a few times that measured on the ground, and concluded that there must be a source of penetrating radiation entering the atmosphere from above.[15] Because of this experiment, Hess is generally credited with the discovery of what Robert Millikan would later dub "cosmic rays".[16]

Although originally thought to be electromagnetic radiation, our modern understanding of cosmic rays is that they are in fact highly energetic charged particles. The vast majority of cosmic rays are protons, but there are also cosmic-ray electrons, positrons, and bare nuclei of helium and heavier elements. The cosmic-ray energy spectrum (particle flux as a function of kinetic energy) is fit rather well by a power-law distribution ($\phi \propto E^{-2.7}$) from 10^{10} eV all the way up to 10^{21} eV (see Fig. 1).[18] This slope and the turn-over in flux that occurs below about 10^{10} eV is consistent for protons and heavier nuclei (*e.g.*, C, O, Fe), suggesting a common origin and acceleration process.[19] Below about 10^9 eV the cosmic-ray flux becomes more difficult to measure as lower-energy particles are deflected from the solar system by the magnetic field coupled to the solar wind, an effect known as modulation. However, as spacecraft such as *Voyager* and *Pioneer* travel farther from the sun and the influence of the solar wind, new data at lower energies (10^7 eV) are continuously acquired.[20]

Because cosmic rays are charged particles, they are deflected by the Galactic magnetic field and do not point back to their places of origin. This makes it impossible to directly pinpoint the sources responsible for particle acceleration. Mounting indirect evidence, however—including energetics arguments and observations tracing the effects of cosmic rays on the ISM—suggest that most Galactic cosmic rays are likely accelerated by the shock waves expanding in supernova remnants through a process known as diffusive shock acceleration.[21]

As cosmic rays propagate away from their sites of acceleration and through the Galaxy,§ they interact with the ISM and the interstellar radiation field in a variety of ways. These include excitation and ionization of atomic and molecular species, the excitation of nuclear states, spallation (fragmentation) of ambient heavy nuclei, the production of neutral pions (π^0) through inelastic collisions, and inverse Compton (IC)

§ When capitalized, "Galaxy" generally refers to our own Milky Way.

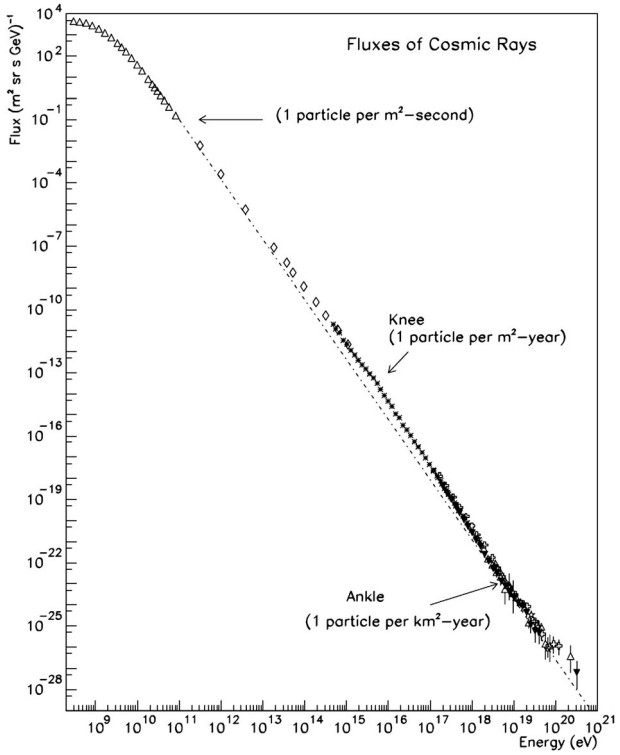

Fig. 1 The all particle spectrum of cosmic rays—prepared by S. P. Swordy for Cronin *et al.* (1997).[17] S. P. Swordy, The Energy Spectra and Anisotropies of Cosmic Rays, *Space Sci. Rev.*, 2001, **99**, 85–94, Fig. 1, © Springer Science + Business Media, with kind permission from Springer Science + Business Media.

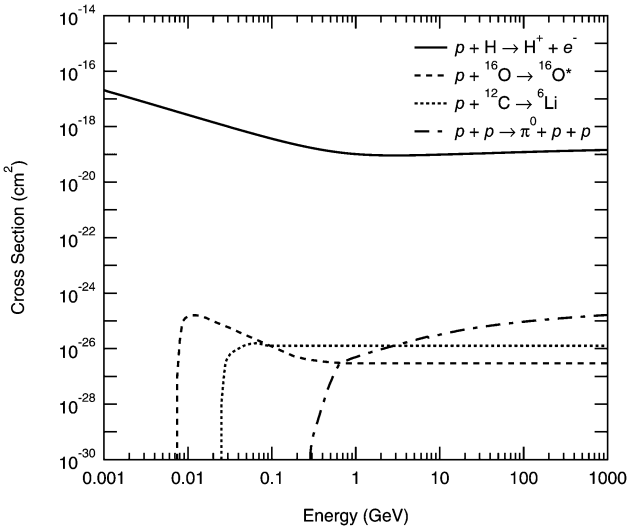

Fig. 2 Cross sections for select processes described in Section 2, including ionization of atomic hydrogen,[24] nuclear excitation of ^{16}O by protons,[26] spallation of ^{12}C by protons to form ^{6}Li,[27] and production of neutral pions from proton–proton collisions.[28]

scattering (Note that some processes are unique to leptonic species, *e.g.*, IC, while others are unique to hadronic species, *e.g.*, π^0 production). All of these interactions leave some observable signature that can be used to infer the presence of cosmic rays: enhanced abundances of molecular ions (*e.g.*, H_3^+, OH^+, HCO^+) from ionization; enhanced ^{6}Li, ^{9}Be, and ^{10}B abundances from spallation; emission of 4.44 MeV and 6.13 MeV gamma-ray lines from the nuclear de-excitation of ^{12}C and ^{16}O, respectively; increased gamma-ray flux near 70 MeV (about one-half of the π^0 rest mass energy) from decay of neutral pions into pairs of photons; increased gamma-ray flux from upscattering of photons on cosmic-ray electrons (IC). The ''strength'' of each observable (*e.g.*, flux of gamma-ray emission, abundance of H_3^+) can be predicted given an adopted cosmic-ray spectrum. This is because the energy dependence of the cross sections for the aforementioned interactions are known (see Fig. 2). The rate of a particular process R_x (*e.g.*, ionization of H_2, formation of ^{9}Be) is given by

$$R_x = 4\pi G_x \int j(E)\sigma_x(E)\mathrm{d}E, \qquad (1)$$

where $j(E)\mathrm{d}E$ is the differential spectrum in terms of protons per unit area per unit time per unit solid angle with kinetic energy in the range $\mathrm{d}E$, $\sigma_x(E)$ is the cross section for process x, and G_x is a coefficient specific to each process (*e.g.*, accounting for ionization by heavier nuclei). Some of the first determinations of the cosmic-ray ionization rate—a parameter important to astrochemical modeling—were made using this method.[22,23] These studies extrapolated the cosmic-ray spectrum observed above ~1 GeV down to lower energies and used the Bethe cross section for the ionization of atomic hydrogen.[24] By numerically integrating the product of both functions over energy, Hayakawa *et al.* (1961)[22] and Spitzer and Tomasko (1968)[23] calculated the cosmic-ray ionization rate of atomic hydrogen, finding $\zeta_H = 10^{-15}$ s^{-1} and $\zeta_H = 7 \times 10^{-18}$ s^{-1}, respectively.

While the integration of eqn (1) is in principle a straightforward calculation, the inferred ionization rates differ by over a factor of 100 due to differences in the authors' extrapolation of the particle spectrum to MeV energies. This is because the cross section for ionization increases with decreasing energy, making protons in the 1–10 MeV range—below the lowest energies where the particle flux has been observed—the most efficient at ionization. Also, these calculations ignore the fact that the distribution of cosmic-ray energies changes as particles propagate into a cloud due to the energy dependence of various interaction cross sections. The larger ionization cross section for low-energy particles means that they will lose energy faster than high-energy particles, and so will be preferentially removed from the spectrum. As a result, as cosmic rays penetrate further and further into a cloud the particles most efficient at ionization are lost and the ionization rate will decrease. Recent studies attempt to account for these effects by computing the particle spectrum as a function of depth into the cloud,[25] but such calculations are beyond the scope of this review.

3 Interstellar chemistry

Of all the processes described above, cosmic-ray ionization is the most important in terms of astrochemistry. Beyond initiating the chain of ion–molecule reactions that drives interstellar

chemistry, ionization has several other relevant effects. Some of these include the energy introduced by the resulting free (often called secondary) electrons, the emission of UV photons from the Lyman and Werner bands of H_2 (excited by secondary electrons), and the desorption of molecules off of grains, as will be discussed below. Because cosmic-ray ionization is so important to astrochemistry, there have been a number of studies devoted to determining the rate at which this process occurs. Many of these studies utilize observations of molecular species that are associated with the beginning steps of ion–molecule chemistry in order to infer the cosmic-ray ionization rate. To understand how this is done, it is necessary to describe some of the relevant background chemistry for several species. Note that the following subset of reactions is far from representing the complete chemistry that occurs in the ISM, and the reader is directed to recent reviews[3,29] if interested in a deeper understanding of ion–molecule chemistry in astrophysical environments.

3.1 Hydrogen chemistry

Probably the simplest example of interstellar chemistry is the purely hydrogenic chemistry surrounding the H_3^+ molecular ion that occurs in diffuse molecular clouds. H_3^+ is formed in a two-step process, beginning with the aforementioned ionization of H_2 by cosmic rays,

$$H_2 + CR \rightarrow H_2^+ + e^- + CR', \quad (2)$$

which is followed by a reaction of H_2^+ with H_2,

$$H_2^+ + H_2 \rightarrow H_3^+ + H. \quad (3)$$

Cosmic-ray ionization is the rate-limiting step in this process (see Table 1 for reaction rate coefficients) and can be taken as the formation rate of H_3^+. In diffuse molecular clouds, H_3^+ is predominantly destroyed *via* dissociative recombination with electrons,

$$H_3^+ + e^- \rightarrow H_2 + H \text{ or } H + H + H. \quad (4)$$

Reactions (2)–(4) are an excellent approximation to the complete chemistry of H_3^+ in the diffuse, molecular ISM. There are, of course, other reactions that can be considered in this chemical scheme, including the dissociative recombination of H_2^+ with electrons,

$$H_2^+ + e^- \rightarrow H + H, \quad (5)$$

and charge transfer between H_2^+ and H,

$$H_2^+ + H \rightarrow H^+ + H_2. \quad (6)$$

However, they do not play major roles in environments where nearly all hydrogen is in the form of H_2 as they are dominated by reaction (3). Reaction (5) requires large electron abundances ($n(e)/n(H_2) > 0.08$) in order to compete with reaction (3), and as long as $n(H_2)/n(H) > 0.31$, H_2^+ will most frequently react with H_2 rather than H.

Similarly, there are numerous alternative destruction pathways for H_3^+ involving various neutral atoms and molecules, *e.g.*,

Table 1 Values below are from the periodically updated list of reaction rate coefficients maintained in the UMIST database for astrochemistry (UDFA), available online at http://www.udfa.net/[30]

Reaction #	Reactants	Rate coefficient ($cm^3\ s^{-1}$)
3	H_2, H_2^+	2.08×10^{-9}
4	H_3^+, e^-	$6.7 \times 10^{-8}\ (T/300)^{-0.51}$
5	H_2^+, e^-	$1.6 \times 10^{-8}\ (T/300)^{-0.43}$
6	H_2^+, H	6.4×10^{-10}
7	H_3^+, CO	1.7×10^{-9}
8	H_3^+, CO	2.7×10^{-11}
9	H_3^+, O	8.4×10^{-10}
10	H_3^+, N_2	1.8×10^{-9}
12	H^+, O	$7.31 \times 10^{-10}\ (T/300)^{0.23} \exp(-225.9/T)$
13	O^+, H_2	1.7×10^{-9}
14	OH^+, H_2	1.01×10^{-9}
16	OH^+, e^-	$3.58 \times 10^{-8}\ (T/300)^{-0.50}$
15	H_2O^+, H_2	6.4×10^{-10}
17	H_2O^+, e^-	$4.3 \times 10^{-7}\ (T/300)^{-0.50}$
18	H_3O^+, e^-	$4.3 \times 10^{-7}\ (T/300)^{-0.50}$
19	H^+, D	$1.0 \times 10^{-9} \exp(-41.0/T)$
20	D^+, H_2	2.1×10^{-9}
21	H_3^+, HD	3.5×10^{-10}
22	H_2D^+, CO	5.7×10^{-10}

$$H_3^+ + CO \rightarrow H_2 + HCO^+, \quad (7)$$

$$H_3^+ + CO \rightarrow H_2 + HOC^+, \quad (8)$$

$$H_3^+ + O \rightarrow H_2 + OH^+, \quad (9)$$

$$H_3^+ + N_2 \rightarrow H_2 + HN_2^+. \quad (10)$$

For typical electron abundances in diffuse clouds ($n(e)/n(H_2) \approx 10^{-4}$) though, dissociative recombination of H_3^+ with electrons is much faster than reactions (7)–(10). As a result, they can be safely omitted from an approximated diffuse cloud chemical network. However, in regions such as dense clouds with much lower electron abundances ($n(e)/n(H_2) \approx 10^{-7}$), these become the dominant pathways by which H_3^+ is destroyed. In fact, it is these very reactions which begin producing larger molecular ions that make H_3^+, and thus ionization by cosmic rays, so important to interstellar chemistry.

3.2 Oxygen chemistry

Ionization of atomic hydrogen by cosmic rays,

$$H + CR \rightarrow H^+ + e^- + CR', \quad (11)$$

is also of great importance to interstellar chemistry. With H^+ present, the chemistry of oxygen bearing species begins with endothermic charge transfer to oxygen to form O^+,

$$H^+ + O + \Delta E \leftrightarrow O^+ + H, \quad (12)$$

where $\Delta E = 226$ K represents the endothermicity of the forward reaction, and the double-sided arrow shows that the exothermic back-reaction proceeds uninhibited. Hydrogen abstraction from H_2 then forms OH^+,

$$O^+ + H_2 \rightarrow OH^+ + H. \quad (13)$$

This chain of hydrogen abstraction reactions can proceed up to H_3O^+, *i.e.*,

$$OH^+ + H_2 \rightarrow H_2O^+ + H, \quad (14)$$

$$H_2O^+ + H_2 \rightarrow H_3O^+ + H, \quad (15)$$

but at every step competes with dissociative recombination with electrons:

$$OH^+ + e^- \rightarrow O + H, \quad (16)$$

$$H_2O^+ + e^- \rightarrow \text{products}, \quad (17)$$

$$H_3O^+ + e^- \rightarrow \text{products}. \quad (18)$$

Two of the products resulting from dissociative recombination of H_3O^+ and H_2O^+ include OH and H_2O, both of which are thought to be primarily formed through this process in the diffuse ISM.

As before, this set of reactions is only an approximation to the interstellar oxygen chemistry in diffuse clouds. Reaction (12) is certainly not the only way in which H^+ is destroyed as protons can also recombine with electrons, react with other neutrals (*e.g.*, reaction (19) below), and stick to small dust grains and PAHs. The importance of these other channels will be discussed in Section 4.1.

3.3 Deuterium chemistry

H^+ can also undergo charge exchange with deuterium,

$$H^+ + D + \Delta E \leftrightarrow D^+ + H, \quad (19)$$

where ΔE = 41 K. This is similar to reaction (12) where the forward reaction is endothermic, while the back-reaction proceeds freely. The resulting D^+ reacts with H_2,

$$D^+ + H_2 \rightarrow H^+ + HD, \quad (20)$$

to form HD. Photodissociation is the primary destruction mechanism of HD in diffuse material. In cold, dense clouds HD reacts with H_3^+,

$$H_3^+ + HD \rightarrow H_2 + H_2D^+, \quad (21)$$

after which deuterium can be incorporated into more complex species through reactions of H_2D^+ with neutrals. One such pathway leads to DCO^+,

$$H_2D^+ + CO \rightarrow DCO^+ + H_2, \quad (22)$$

which, along with its non-deuterated counterpart HCO^+, has been observed in dense clouds. Because deuterated species are linked to ionization of both H and H_2, their abundances are useful in constraining the cosmic-ray ionization rate.

3.4 Caveats

It should be apparent by now that several considerations must be taken into account when determining which reactions are driving interstellar chemistry. Despite the simple reaction schemes presented above, there are numerous reactions not given that can form and destroy all of the species under consideration. For example, the UMIST database for astrochemistry[30] includes almost 20 formation pathways and 50 destruction pathways for OH^+. In diffuse clouds the main channel leading to OH^+ is reactions (12) and (13), while in dense clouds reaction (9) dominates.[31] The key lies in knowing which reactions must be included and which can be ignored under various circumstances. That said, in most cases a reasonable approximation to interstellar chemistry for particular conditions can be represented by a handful of the most important reactions.

4 Inferring the cosmic-ray ionization rate

It is worth noting here that many times different studies are actually calculating slightly different ionization rates. These include: (i) the primary ionization rate (ζ_p) which is the ionization rate of atomic hydrogen due only to cosmic-ray particles (protons and heavy nuclei); (ii) the total ionization rate of atomic hydrogen (ζ_H) which is the ionization rate of atomic hydrogen due to cosmic-rays and energetic secondary electrons produced *via* ionization; (iii) the total ionization rate of molecular hydrogen (ζ_2) which is the ionization rate of molecular hydrogen due to cosmic-rays and energetic secondary electrons produced *via* ionization. Approximate expressions relating the different ionization rates are $\zeta_H = 1.5\zeta_p$ and $\zeta_2 = 2.3\zeta_p$.[32] These relations account for differences in the ionization cross sections for H and H_2, as well as the expected contribution from secondary electrons. When comparing ionization rates from different studies, it is always necessary to determine which ionization rate is being reported. This is sometimes made more difficult by the lack of convention for notation, and the occasional lack of any identifying mark beyond ζ.

Calculating the ionization rate from molecular abundances is based on the chemical pathways described above. The basic premise is that the rate of change of the abundance of any species can be written as a differential equation that accounts for formation and destruction mechanisms, *e.g.*,

$$\frac{d}{dt}n(H_3^+) = n(H_2^+)n(H_2)k_3 - n(H_3^+)n(e)k_4, \quad (23)$$

where $n(H_2^+)n(H_2)k_3$ gives the formation rate of H_3^+ and $n(H_3^+)n(e)k_4$ gives the destruction rate of H_3^+. Here, $n(X)$s are number densities of species X, and k_is are reaction rate coefficients.¶ The inclusion of other formation or destruction mechanisms simply requires the addition of more terms (*e.g.*, $-n(H_3^+)n(O)k_9$ in the case of reaction (9)). Note that this means expressions like these are *always* approximations to the complete chemistry as more formation and destruction mechanisms can be added. For simple analytic expressions steady-state is typically assumed, making the left-hand side of the equation equal to 0. This sets the formation and destruction rates equal to each other:

$$n(H_2^+)n(H_2)k_3 = n(H_3^+)n(e)k_4. \quad (24)$$

Assuming that hydrogen is predominantly in molecular form, steady-state for H_2^+ is given by

$$\zeta_2 n(H_2) = n(H_2^+)n(H_2)k_3, \quad (25)$$

¶ The subscript i denotes the reaction number in this paper.

and $\zeta_2 n(H_2)$ can be substituted for the left-hand side of eqn (24) resulting in

$$\zeta_2 n(H_2) = n(H_3^+) n(e) k_4, \quad (26)$$

which can then be re-arranged to solve for the ionization rate. Additionally, substitutions are made to put the equation in terms of variables that are more easily determined, such as the electron fraction (defined as $x_e \equiv n(e)/n_H$, where $n_H \equiv n(H) + 2n(H_2)$) resulting in

$$\zeta_2 = k_4 x_e n_H \frac{n(H_3^+)}{n(H_2)}. \quad (27)$$

Observations cannot measure changes in these parameters along a line-of-sight, so many times a uniform cloud with path length L and constant x_e, k_4, and number densities are assumed. In this case, the H_3^+ and H_2 number densities can by definition be replaced with column densities‖ $N(H_3^+)/L$ and $N(H_2)/L$, respectively, such that

$$\zeta_2 = k_4 x_e n_H \frac{N(H_3^+)}{N(H_2)} \quad (28)$$

gives the cosmic-ray ionization rate in a diffuse molecular cloud. Similar steady state analyses can be applied to other species (*e.g.*, OH, HD, OH^+, HCO^+, H_3O^+) with the same intent of inferring the ionization rate.

4.1 Diffuse clouds

The earliest estimates of the cosmic-ray ionization rate utilizing molecular abundances were based on observations of OH and HD in diffuse molecular clouds. Because these studies rely on oxygen and deuterium chemistries, both of which begin with ionization of atomic hydrogen, the ionization rates determined therein are total ionization rates of atomic hydrogen, ζ_H. HD column densities were determined *via* observations of electronic transitions out of the ground state near 106 nm using *Copernicus*—a space-based UV observatory—while OH column densities were determined from ground-based observations of electronic transitions near 380 nm, again from the ground state. With these measured column densities, the reaction schemes presented above, and reaction rate coefficients from the literature, ionization rates of typically a few times 10^{-17} s^{-1} were inferred in the diffuse, molecular ISM.[33–35] Later studies utilizing OH and HD continued to find ionization rates on the order of a few times 10^{-17} s^{-1},[36] in good agreement with updated estimates of $\zeta_H = (3–4) \times 10^{-17}$ s^{-1} from the cosmic-ray spectrum measured by *Voyager*.[20] As a result, it was generally thought that the cosmic-ray ionization rate was relatively uniform throughout the Galaxy, and a canonical value of $\zeta_H = 3 \times 10^{-17}$ s^{-1} was frequently adopted in the literature when necessary for other calculations.

‖ Column density is defined as $N(X) \equiv \int n(X)\, dL$, and gives the total number of molecules (or atoms) in a pencil beam along the integrated line of sight between the background source and observer per unit area, typically cm^{-2}. It is a useful quantity as it is directly related to the strength of absorption lines and easily calculated from observations.

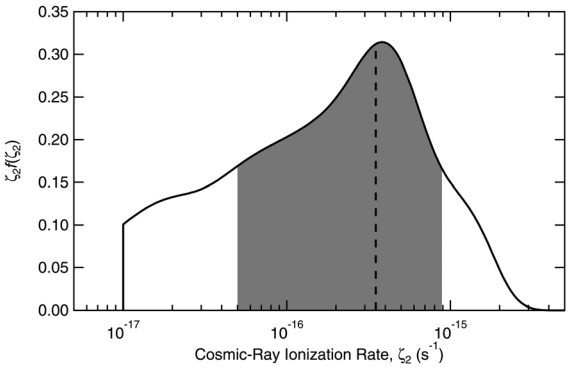

Fig. 3 Reproduction of a portion of Fig. 16 in Indriolo and McCall (2012)[40] showing the distribution of cosmic-ray ionization rates. The product $\zeta_2 f(\zeta_2)$ allows one to see ''by eye'' what portion of the probability density function ($f(\zeta_2)$) carries the largest weight given the logarithmic axis. The mean ionization rate, 3.5×10^{-16} s^{-1}, is marked by the dashed line, and the shaded region is the smallest range of ionization rates in log space that contains 68.3% of the area (1σ equivalent) under the probability density function.

The detection of H_3^+ in the ISM[37] brought a new, less complicated tracer of the ionization rate of molecular hydrogen to the stage, and initial results showed an ionization rate over one order of magnitude larger than previously thought.[38] This was especially striking because ionization rates determined from OH and H_3^+ *in the same sight line*** differed by a factor of ~15.[39] Most recently, a survey of H_3^+ in 50 diffuse molecular cloud sight lines was used to determine the distribution of ionization rates in the local region of the Galaxy, resulting in a mean ionization rate of $\zeta_2 = 3.5 \times 10^{-16}$ s^{-1}, and 68.3% probability (1σ equivalent) of ionization rates between 0.5×10^{-16} s^{-1} and 8.8×10^{-16} s^{-1},[40] as shown in Fig. 3. The two most important findings from this study are the confirmation of a higher mean ionization rate (a few times 10^{-16} s^{-1} is now widely accepted as a typical value in diffuse clouds), and the wide distribution of ionization rates with values as high as 10^{-15} s^{-1}, and 3σ upper limits as low as 3×10^{-17} s^{-1} that suggest variations in the underlying cosmic-ray spectrum.

This brief historical review on the cosmic-ray ionization rate as inferred from molecular abundances (see Dalgarno 2006[41] for a more in-depth review on the subject) is instructive for demonstrating the pitfalls that can arise when approximating interstellar chemistry with simple analytical expressions. If the chemical networks associated with hydrogen, oxygen, and deuterium chemistry were fully described by the reactions presented in Section 3, there should be no differences in the ionization rates inferred from different species. As we have already indicated though, there are many more reactions aside from those included in this paper. Charge transfers from H^+ to O and D (reactions (12) and (19), respectively) are of chief importance to the formation of OH and HD, but neutralization of H^+ on PAHs and small grains is highly competitive with these

** The sight line in question here is that toward the background star HD 24398—also commonly known as ζ Persei—a bright star well studied at many wavelengths with column densities measured for several atomic and molecular species.

processes.[31,42] The removal of H^+ makes the reaction network between the ionization of atomic hydrogen and the formation of OH and HD "leaky", and was a mechanism not considered by the studies utilizing these species to infer ζ_H. It was realized by Liszt (2003)[42] that accounting for neutralization of H^+ on grains could reconcile the differences in ionization rates inferred from H_3^+ *versus* OH and HD, as larger values of ζ_H are necessary to produce the observed OH and HD abundances when a significant fraction of H^+ is removed from the chemical network.

Recently, observations of OH^+ and H_2O^+ in a diffuse cloud toward the background source W51 made with the *Herschel Space Observatory* were used in concert with H_3^+ observations in the same cloud so that ionization rates could be calculated using both the hydrogen and oxygen chemical networks.[43] The ionization rate inferred from H_3^+ was about 14 times larger than that inferred from OH^+ and H_2O^+ (when H^+ neutralization on grains is naively ignored), similar to the aforementioned discrepancy found using H_3^+ and OH, suggesting that only about 7% of the time does cosmic-ray ionization of atomic hydrogen lead to OH^+. By calibrating the relationship between ionization rates inferred from H_3^+ and from other species, these other species can then be used independently to determine ionization rates in regions where H_3^+ cannot be observed. This is of particular importance given the wealth of recent OH^+ and H_2O^+ observations in diffuse, mostly atomic clouds made with *Herschel*.[44,45]

4.2 Dense clouds

In regions of higher density the destruction of molecules by photodissociation is minimized due to the severly attenuated UV field, and timescales for collisions become much shorter, enabling the formation of more complex species. With more potential reaction partners, chemistry in dense clouds is more complicated than in diffuse clouds, making it difficult to infer the ionization rate from simple analytical expressions. Instead, most studies rely on chemical models using different combinations of input parameters (*e.g.*, density, temperature, ionization rate), comparing predicted abundance ratios to those observed to determine the best-fit physical conditions. A common set of species observed for this purpose includes HCO^+, DCO^+, and CO, with the ratios $n(HCO^+)/n(CO)$ and $n(DCO^+)/n(HCO^+)$ being sensitive to the ionization rate and electron fraction. Ionization rates determined from observations of these molecules in dense cloud cores are typically in the range 10^{-18} s^{-1} $\leq \zeta_2 \leq$ 10^{-16} s^{-1},[46,47] lower than found in diffuse clouds. This result is consistent with the picture described in Section 2 where the ionization rate should decrease deeper inside clouds due to the loss of lower-energy particles. Ranges†† of 1 MeV, 10 MeV, and 100 MeV protons are 2.5×10^{20} cm^{-2}, 1.6×10^{22} cm^{-2}, and 1.2×10^{24} cm^{-2}, respectively,[48] and average column densities in diffuse clouds are on the order of 10^{21} cm^{-2}, while average column densities in dense clouds are on the order of 10^{23} cm^{-2}. As such, the difference in ionization rates between diffuse and dense clouds is likely explained by a scenario where the interiors of diffuse clouds experience a larger cosmic-ray flux than the interiors of dense clouds which cannot be reached by low-energy particles.

†† Given here as the column density through which a particle can travel before losing all of its energy to ionization interactions.

5 Further influence of cosmic-rays on astrochemistry

We have shown above that certain molecular abundances are highly dependent on the cosmic-ray ionization rate due to their close association with ion–molecule chemistry. Beyond these species though, there are more subtle effects that cosmic rays have on astrochemistry which warrant discussion.

Although cosmic-ray ionization of hydrogen is most important for initiating the web of ion–molecule reactions, ionization of helium can also affect the chemistry in dense clouds. In such regions nearly all carbon is driven into CO, effectively inhibiting the development of more complex carbon-based molecules. However, reaction of CO with He^+,

$$He^+ + CO \rightarrow He + C^+ + O, \quad (29)$$

frees some amount carbon in the form of C^+, which can then start a chain of reactions leading to methane or acetylene.[29] This process can be especially important in the envelopes of gas surrounding newly forming stars where the warm ($T \approx$ 200–500 K) conditions and high densities can drive endothermic reactions such as

$$C^+ + H_2 \rightarrow CH^+ + H, \quad (30)$$

that would not proceed in colder regions.

The interiors of dense, starless cloud cores and the midplanes of protoplanetary disks are some of the coldest ($T \sim$ 10 K), most heavily extincted astrophysical environments. Essentially no external UV or X-ray radiation reaches these regions, and most molecules are incorporated into ice mantles on interstellar grains (so-called "freeze out") inhibiting the progression of gas-phase chemistry. As higher-energy cosmic rays can penetrate to the interiors of dense clouds and disks, they provide an important source of input energy. Ionization of H_2 releases free electrons that—on average—have kinetic energies of about 30 eV.[48] Collisions between these electrons and ambient material can serve to heat the gas and grains. Additionally, collisions with energetic electrons can excite the Lyman and Werner bands of H_2, which then emit UV photons.[49] This mechanism is expected to be the dominant source of ionizing photons inside such dense regions, and the induced UV field can both dissociate and desorb molecules frozen onto grain surfaces. Direct cosmic-ray impacts on grains can also desorb molecules, and both cosmic-ray desorption and cosmic-ray induced photodesorption are two processes possibly responsible for maintaining small gas-phase populations of some molecules in disk midplanes and dense cores.

Cosmic-ray induced photodissociation of molecules frozen onto grains is also thought to be important for grain–surface chemistry.[14] Radicals produced on the icy grain mantle can

migrate across the surface—if the temperature is high enough—leading to the formation of more complex species. The warmer temparatures around newly forming stars facilitate surface migration, and can vastly increase the chemical complexity in these regions.

6 Observable effects of cosmic-rays

As discussed in Section 2, cosmic rays interact with the interstellar medium in a multitude of ways, all of which potentially produce observable effects. Not only do these observables indicate the presence of cosmic rays, but they can also be useful in constraining the cosmic-ray energy spectrum and ionization rate.

6.1 X-ray line emission from electronic de-excitation

While cosmic rays most frequently ionize H and H_2, simply because hydrogen is so much more abundant than any other element, they can also ionize every other species in the ISM. When ionization frees an electron from the innermost ($n = 1$) shell of an atom, the vacancy is quickly filled *via* electronic transition from a higher level, resulting in the emission of a photon. For example, the transition from $n = 2$ to $n = 1$ in iron—known as Fe Kα—emits an X-ray photon at 6.4 keV. The strength of this emission line can be used to determine the rate at which Fe is ionized, although it does not differentiate between ionization by photons, hadronic cosmic rays, and leptonic cosmic rays. Iron is found in all phases of the ISM (*i.e.*, not confined to clouds shielded from X-rays), and Fe Kα emission is most commonly seen in regions known for both high X-ray and particle fluxes (*e.g.*, the Galactic center), making it difficult to disentangle the contribution from each. Still, one recent study used observations of the Fe Kα line near the Arches cluster‡‡ to estimate a cosmic-ray ionization rate of 10^{-13} s^{-1}, much higher than found anywhere else in the Galaxy.[50]

6.2 Gamma-ray emission from π^0 decay

Inelastic collisions between hadronic cosmic rays and ambient nuclei can result in the production of neutral pions:

$$p + p \rightarrow p + p + \pi^0. \quad (31)$$

The mean lifetime of a π^0 is incredibly short—about 10^{-16} s—and the dominant decay mode (99% of the time) is a pair of gamma-ray photons,[51] meaning gamma-ray flux can be related to cosmic-ray flux. The material in molecular clouds presents a wealth of ''targets'' for cosmic-ray protons, such that molecular clouds are expected to be sources of gamma-ray emission. One of the most exciting recent developments in tracing the effects of cosmic-ray interactions with the ISM has been the detection§§ of gamma-ray sources that coincide with molecular clouds.[52]

‡‡ Large cluster of young, high mass, high luminosity stars near the Galactic center.

§§ The current generation of gamma-ray observatories operating at GeV and TeV energies includes *Fermi*-LAT, *MAGIC*, *VERITAS*, and H.E.S.S.

Gamma-ray emission is also seen from molecular clouds that are known to be interacting with supernova remnants. Although it is difficult to determine what portion of the gamma-ray emission comes from π^0 decay, inverse Compton scattering, and/or bremsstrahlung, many supernova remnants also show synchrotron emission at radio wavelengths due to relativistic electrons (see Section 6.5 for a discussion on the electron interactions). Using models to simultaneously reproduce both the radio and gamma-ray emission spectra, it seems clear in many cases that the gamma-ray emission does indeed come from π^0 decay, thus indicating that supernova remnants efficiently accelerate both leptonic and hadronic particles.

6.3 Gamma-ray line emission from nuclear de-excitation

Just as cosmic rays can excite electronic states in atoms and molecules, they can also excite nuclear states. The de-excitation of these states results in gamma-ray photons emitted at specific energies. For example, de-excitation in ^{12}C will emit a 4.44 MeV photon, in ^{16}O will emit a 6.13 MeV photon, and in ^{20}Ne will emit a 1.63 MeV photon. As oxygen, carbon, and neon are the third, fourth, and fifth most abundant atomic species in the universe (following hydrogen and helium),[53] there are ample targets for cosmic rays. The thresholds for exciting these nuclear states are in the few MeV range (*e.g.*, see Fig. 2), making observations of these gamma-ray lines potentially powerful probes of the low-energy cosmic-ray flux. Unfortunately, to date these gamma-ray lines have never been detected. Recent estimates of the line flux expected from the inner Galaxy are below the detection sensitivities of the International Gamma-Ray Astrophysics Laboratory (INTEGRAL), at present the most sensitive observatory that operates in this energy range.[54] However, it is likely that the next generation of gamma-ray telescopes will be able to detect these nuclear de-excitation lines, adding a unique constraint to the low-energy cosmic-ray flux.

6.4 Light element isotope abundances

Aside from exciting nuclear states in heavy atoms, cosmic rays can also fragment heavy atoms into smaller pieces (a process called spallation). The most common of these interactions are proton and alpha particle (helium nucleus) cosmic rays spalling carbon, nitrogen, and oxygen nuclei,

$$(p,\alpha) + (C,N,O) \rightarrow (^6Li,^7Li,^9Be,^{10}B,^{11}B), \quad (32)$$

resulting in different isotopes of the light elements lithium, beryllium, and boron. Also, α particle fusion reactions,

$$\alpha + {}^4He \rightarrow (^6Li,^7Li), \quad (33)$$

can generate either of the lithium isotopes. Despite their small sizes, Li, Be, and B are some of the least abundant elements in the universe—about 10 orders of magnitude less abundant than hydrogen. While some amount of ^7Li was produced through nucleosynthesis shortly after the big bang, and both ^7Li and ^{11}B can be produced in supernova explosions, the other three isotopes are thought to only form *via* cosmic-ray spallation. This means that the abundances of ^6Li, ^9Be, and ^{10}B can be useful in tracing the cosmic-ray flux. However, observed

absolute abundances of these isotopes depend on many factors, including the abundances of C, N, and O throughout the history of the Galaxy, the cosmic-ray flux throughout the history of the Galaxy, and the possibility for incorporation into and destruction within stars. The *relative* abundances of these species though should say something about the time-averaged shape of the cosmic-ray spectrum near the energy thresholds at which the relevant spallation interactions ''turn on''. Indeed, certain functional forms of the low-energy cosmic-ray spectrum are likely ruled out because they do not reproduce the observed ^{6}Li/^{9}Be and ^{10}B/^{9}Be abundance ratios.[55]

6.5 Inverse compton, synchrotron, and bremsstrahlung

Cosmic-ray electrons are also responsible for generating various observables, primarily high or low energy photons, through mechanisms such as inverse Compton scattering, bremsstrahlung, and synchrotron. As described above, inverse Compton scattering is a process by which photons—primarily photons from the Cosmic Microwave Background—interact with relativistic electrons, gaining energy in the process. As photons pass through a region with a high concentration of energetic electrons, many will be upscattered to gamma-ray energies, thus providing a signature of the cosmic-ray electrons. Bremsstrahlung—literally ''braking radiation''—results when a charged particle, generally an electron, is deflected by the electric field of an ambient nucleus. While all electrons emit bremsstrahlung radiation, the resulting spectrum is different for thermal (*e.g.*, hot plasma) *versus* non-thermal (cosmic rays) energy distributions, making it possible to distinguish the signatures of each. Finally, synchrotron radiation is the result of charged particles spiraling about magnetic field lines in the ISM. Electrons lose energy to this mechanism much faster than protons, meaning that observed synchrotron radiation is dominated by electrons. Given a population of energetic electrons, all three of the above processes *will* occur. Readers interested in more details on the subject are directed to a review[56] that discusses inverse Compton, bremsstrahlung, and synchrotron radiation, how the different mechanisms depend on the underlying distribution of electron energies, and what radio, X-ray, and gamma-ray observations of supernova remnants reveal about electron acceleration.

6.6 Constraining the cosmic-ray flux

With so many observable effects revealing the presence of energetic particles, it should be possible to use a suite of observations in determining the cosmic-ray energy spectrum. Molecular abundances, light element isotopes, gamma-ray flux, X-ray flux, radio flux: all depend on the spectrum of cosmic rays, and all in different ways because of the energy dependent cross sections. Ionization and nuclear de-excitation trace particles with MeV energies; spallation, particles with energies on the order of tens of MeV; pion production, particles with energies on the order of hundreds of MeV and higher. By observing all of these tracers, the underlying proton spectrum can be reconstructed piece by piece. With the addition of synchrotron, bremsstrahlung, and inverse Compton observations, the importance of protons *versus* electrons can be constrained. While no study taking advantage of all of these tracers has yet been made, the next generation of telescopes and instruments at relevant energies should bring such a possiblilty to light.

7 Summary

The goal of this tutorial review has been to outline our modern understanding of cosmic rays, examine the many ways in which energetic particles interact with interstellar matter, describe the potential observable signatures produced by these interactions, and provide an overview of the effects that cosmic rays have on the chemistry and chemical makeup in astrophysical environments. With that in mind, we briefly review some of the key points discussed herein.

1. Chemistry in astrophysical environments is primarily driven by fast ion–molecule reactions. Photoionization is only efficient for species with ionization potentials below that of atomic hydrogen (13.6 eV), while cosmic rays can ionize any species in any location. As a result, it is thought that cosmic-ray ionization is vital to initiating chemical reaction networks throughout the ISM.

2. Observed abundances of certain molecular ions, such as H_3^+, OH^+, H_2O^+, HCO^+, and DCO^+, can be used to infer the cosmic-ray ionization rate. Current findings show average ionization rates to be about 10 times larger in diffuse clouds than in dense clouds, and both environments show distributions of ionization rates spanning 1–2 orders of magnitude.

3. In environments that photons cannot penetrate, cosmic rays provide a source of input energy by freeing electrons and inducing an internal UV field through the excitation of H_2. These effects can be important for driving chemistry on grain surfaces, a process likely important to producing the chemical diversity observed in regions where young stars are forming.

4. Isotopes of the light elements lithium, beryllium, and boron are produced *via* cosmic-ray spallation of heavier nuclei in the ISM. In the case of ^{9}Be this is thought to be the sole production mechanism, meaning all beryllium on Earth is the result of cosmic-ray spallation—an example of just how close to home we can see the effects that cosmic rays have on chemistry.

5. Cosmic-ray protons and electrons can interact with interstellar matter to produce gamma rays *via* π^0 decay and bremsstrahlung, respectively. Electrons can also interact with the radiation field through inverse Compton scattering, turning low-energy photons into high-energy photons. Gamma-ray observations of supernova remnants indicate that all of these processes are occuring, supporting the picture of remnants as cosmic-ray accelerators.

As larger telescopes are built, more sensitive instruments are designed, and new transitions are identified through laboratory spectroscopy, the list of molecules detected in the ISM will continue to grow. At the same time, laboratory work is improving the accuracy of reaction rate coefficients, and model chemical reaction networks are growing ever more complex to incorporate different physical effects. The combination of all of

these developments presents an exciting prospect, where the entire inventory of observed molecules is used in unison to constrain the cosmic-ray ionization rate and other physical parameters. Certainly, the future intertwining of astrochemistry and particle astrophysics is looking bright.

The authors thank the anonymous referees for comments and suggestions that significantly improved this manuscript. N.I. was funded by NASA Research Support Agreement No. 1393741 provided through JPL.

References

1 C. F. McKee, *The Physics of the Interstellar Medium and Intergalactic Medium*, 1995, p. 292.
2 K. M. Ferrière, *Rev. Mod. Phys.*, 2001, **73**, 1031–1066.
3 T. P. Snow and B. J. McCall, *Annu. Rev. Astron. Astrophys.*, 2006, **44**, 367–414.
4 C. F. McKee and J. P. Ostriker, *Astrophys. J.*, 1977, **218**, 148–169.
5 M. G. Wolfire, D. Hollenbach, C. F. McKee, A. G. G. M. Tielens and E. L. O. Bakes, *Astrophys. J.*, 1995, **443**, 152–168.
6 M. G. Wolfire, C. F. McKee, D. Hollenbach and A. G. G. M. Tielens, *Astrophys. J.*, 2003, **587**, 278–311.
7 N. J. Evans, II, *Annu. Rev. Astron. Astrophys.*, 1999, **37**, 311–362.
8 C. F. McKee and E. C. Ostriker, *Annu. Rev. Astron. Astrophys.*, 2007, **45**, 565–687.
9 R. C. Kennicutt and N. J. Evans, *Annu. Rev. Astron. Astrophys.*, 2012, **50**, 531–608.
10 A. G. G. M. Tielens, *The Physics and Chemistry of the Interstellar Medium*, Cambridge University Press, Cambridge, 2005.
11 D. E. Osterbrock and G. J. Ferland, *Astrophysics of gaseous nebulae and active galactic nuclei*, University Science Books, 2006.
12 E. Herbst and W. Klemperer, *Astrophys. J.*, 1973, **185**, 505–534.
13 W. D. Watson, *Astrophys. J.*, 1973, **183**, L17.
14 R. T. Garrod, S. L. W. Weaver and E. Herbst, *Astrophys. J.*, 2008, **682**, 283–302.
15 V. F. Hess, *Phys. Z.*, 1912, **13**, 1084.
16 R. A. Millikan, *Proc. Natl. Acad. Sci. U. S. A.*, 1926, **12**, 48–55.
17 J. W. Cronin, T. K. Gaisser and S. P. Swordy, *Science*, 1997, **276**, 32–37.
18 S. P. Swordy, *Space Sci. Rev.*, 2001, **99**, 85–94.
19 H. S. Ahn, P. Allison, M. G. Bagliesi, L. Barbier, J. J. Beatty, G. Bigongiari, T. J. Brandt, J. T. Childers, N. B. Conklin, S. Coutu, M. A. Du Vernois, O. Ganel, J. H. Han, J. A. Jeon, K. C. Kim, M. H. Lee, P. Maestro, A. Malinine, P. S. Marrocchesi, S. Minnick, S. I. Mognet, S. W. Nam, S. Nutter, I. H. Park, N. H. Park, E. S. Seo, R. Sina, P. Walpole, J. Wu, J. Yang, Y. S. Yoon, R. Zei and S. Y. Zinn, *Astrophys. J.*, 2009, **707**, 593–603.
20 W. R. Webber, *Astrophys. J.*, 1998, **506**, 329–334.
21 L. O. Drury, *Rep. Prog. Phys.*, 1983, **46**, 973–1027.
22 S. Hayakawa, S. Nishimura and T. Takayanagi, *Publ. Astron. Soc. Jpn.*, 1961, **13**, 184.
23 L. Spitzer, Jr. and M. G. Tomasko, *Astrophys. J.*, 1968, **152**, 971.
24 H. Bethe, *Handbuch der Physik*, Springer, Berlin, 1933, vol. 24 (Pt. 1).
25 M. Padovani, D. Galli and A. E. Glassgold, *Astron. Astrophys.*, 2009, **501**, 619–631.
26 R. Ramaty, B. Kozlovsky and R. E. Lingenfelter, *Astrophys. J., Suppl. Ser.*, 1979, **40**, 487–526.
27 S. M. Read and V. E. Viola, Jr., *At. Data Nucl. Data Tables*, 1984, **31**, 359.
28 C. D. Dermer, *Astrophys. J.*, 1986, **307**, 47–59.
29 M. Larsson, W. D. Geppert and G. Nyman, *Rep. Prog. Phys.*, 2012, **75**, 066901.
30 D. McElroy, C. Walsh, A. J. Markwick, M. A. Cordiner, K. Smith and T. J. Millar, *Astron. Astrophys.*, 2013, **550**, A36.
31 D. Hollenbach, M. J. Kaufman, D. Neufeld, M. Wolfire and J. R. Goicoechea, *Astrophys. J.*, 2012, **754**, 105.
32 A. E. Glassgold and W. D. Langer, *Astrophys. J.*, 1974, **193**, 73–91.
33 E. J. O'Donnell and W. D. Watson, *Astrophys. J.*, 1974, **191**, 89–92.
34 J. H. Black and A. Dalgarno, *Astrophys. J., Suppl. Ser.*, 1977, **34**, 405–423.
35 T. W. Hartquist, H. T. Doyle and A. Dalgarno, *Astron. Astrophys.*, 1978, **68**, 65–67.
36 S. R. Federman, J. Weber and D. L. Lambert, *Astrophys. J.*, 1996, **463**, 181.
37 T. R. Geballe and T. Oka, *Nature*, 1996, **384**, 334–335.
38 B. J. McCall, A. J. Huneycutt, R. J. Saykally, T. R. Geballe, N. Djuric, G. H. Dunn, J. Semaniak, O. Novotny, A. Al-Khalili, A. Ehlerding, F. Hellberg, S. Kalhori, A. Neau, R. Thomas, F. Österdahl and M. Larsson, *Nature*, 2003, **422**, 500–502.
39 N. Indriolo, T. R. Geballe, T. Oka and B. J. McCall, *Astrophys. J.*, 2007, **671**, 1736–1747.
40 N. Indriolo and B. J. McCall, *Astrophys. J.*, 2012, **745**, 91.
41 A. Dalgarno, *Proc. Natl. Acad. Sci. U. S. A.*, 2006, **103**, 12269–12273.
42 H. Liszt, *Astron. Astrophys.*, 2003, **398**, 621–630.
43 N. Indriolo, D. A. Neufeld, M. Gerin, T. R. Geballe, J. H. Black, K. M. Menten and J. R. Goicoechea, *Astrophys. J.*, 2012, **758**, 83.
44 M. Gerin, M. de Luca, J. Black, J. R. Goicoechea, E. Herbst, D. A. Neufeld, E. Falgarone, B. Godard, J. C. Pearson, D. C. Lis, T. G. Phillips, T. A. Bell, P. Sonnentrucker, F. Boulanger, J. Cernicharo, A. Coutens, E. Dartois, P. Encrenaz, T. Giesen, P. F. Goldsmith, H. Gupta, C. Gry, P. Hennebelle, P. Hily-Blant, C. Joblin, M. Kazmierczak, R. Kolos, J. Krelowski, J. Martin-Pintado, R. Monje, B. Mookerjea, M. Perault, C. Persson, R. Plume, P. B. Rimmer, M. Salez, M. Schmidt, J. Stutzki, D. Teyssier, C. Vastel, S. Yu, A. Contursi, K. Menten, T. Geballe, S. Schlemmer, R. Shipman, A. G. G. M. Tielens, S. Philipp-May, A. Cros, J. Zmuidzinas, L. A. Samoska, K. Klein and A. Lorenzani, *Astron. Astrophys.*, 2010, **518**, L110.

45 D. A. Neufeld, J. R. Goicoechea, P. Sonnentrucker, J. H. Black, J. Pearson, S. Yu, T. G. Phillips, D. C. Lis, M. de Luca, E. Herbst, P. Rimmer, M. Gerin, T. A. Bell, F. Boulanger, J. Cernicharo, A. Coutens, E. Dartois, M. Kazmierczak, P. Encrenaz, E. Falgarone, T. R. Geballe, T. Giesen, B. Godard, P. F. Goldsmith, C. Gry, H. Gupta, P. Hennebelle, P. Hily-Blant, C. Joblin, R. Kołos, J. Krełowski, J. Martín-Pintado, K. M. Menten, R. Monje, B. Mookerjea, M. Perault, C. Persson, R. Plume, M. Salez, S. Schlemmer, M. Schmidt, J. Stutzki, D. Teyssier, C. Vastel, A. Cros, K. Klein, A. Lorenzani, S. Philipp, L. A. Samoska, R. Shipman, A. G. G. M. Tielens, R. Szczerba and J. Zmuidzinas, *Astron. Astrophys.*, 2010, **521**, L10.
46 P. Caselli, C. M. Walmsley, R. Terzieva and E. Herbst, *Astrophys. J.*, 1998, **499**, 234.
47 J. P. Williams, E. A. Bergin, P. Caselli, P. C. Myers and R. Plume, *Astrophys. J.*, 1998, **503**, 689.
48 T. E. Cravens and A. Dalgarno, *Astrophys. J.*, 1978, **219**, 750–752.
49 S. S. Prasad and S. P. Tarafdar, *Astrophys. J.*, 1983, **267**, 603–609.
50 V. Tatischeff, A. Decourchelle and G. Maurin, *Astron. Astrophys.*, 2012, **546**, A88.
51 J. Beringer, J.-F. Arguin, R. M. Barnett, K. Copic, O. Dahl, D. E. Groom, C.-J. Lin, J. Lys, H. Murayama, C. G. Wohl, W.-M. Yao, P. A. Zyla, C. Amsler, M. Antonelli, D. M. Asner, H. Baer, H. R. Band, T. Basaglia, C. W. Bauer, J. J. Beatty, V. I. Belousov, E. Bergren, G. Bernardi, W. Bertl, S. Bethke, H. Bichsel, O. Biebel, E. Blucher, S. Blusk, G. Brooijmans, O. Buchmueller, R. N. Cahn, M. Carena, A. Ceccucci, D. Chakraborty, M.-C. Chen, R. S. Chivukula, G. Cowan, G. D'Ambrosio, T. Damour, D. de Florian, A. de Gouvêa, T. DeGrand, P. de Jong, G. Dissertori, B. Dobrescu, M. Doser, M. Drees, D. A. Edwards, S. Eidelman, J. Erler, V. V. Ezhela, W. Fetscher, B. D. Fields, B. Foster, T. K. Gaisser, L. Garren, H.-J. Gerber, G. Gerbier, T. Gherghetta, S. Golwala, M. Goodman, C. Grab, A. V. Gritsan, J.-F. Grivaz, M. Grünewald, A. Gurtu, T. Gutsche, H. E. Haber, K. Hagiwara, C. Hagmann, C. Hanhart, S. Hashimoto, K. G. Hayes, M. Heffner, B. Heltsley, J. J. Hernández-Rey, K. Hikasa, A. Höcker, J. Holder, A. Holtkamp, J. Huston, J. D. Jackson, K. F. Johnson, T. Junk, D. Karlen, D. Kirkby, S. R. Klein, E. Klempt, R. V. Kowalewski, F. Krauss, M. Kreps, B. Krusche, Y. V. Kuyanov, Y. Kwon, O. Lahav, J. Laiho, P. Langacker, A. Liddle, Z. Ligeti, T. M. Liss, L. Littenberg, K. S. Lugovsky, S. B. Lugovsky, T. Mannel, A. V. Manohar, W. J. Marciano, A. D. Martin, A. Masoni, J. Matthews, D. Milstead, R. Miquel, K. Mönig, F. Moortgat, K. Nakamura, M. Narain, P. Nason, S. Navas, M. Neubert, P. Nevski, Y. Nir, K. A. Olive, L. Pape, J. Parsons, C. Patrignani, J. A. Peacock, S. T. Petcov, A. Piepke, A. Pomarol, G. Punzi, A. Quadt, S. Raby, G. Raffelt, B. N. Ratcliff, P. Richardson, S. Roesler, S. Rolli, A. Romaniouk, L. J. Rosenberg, J. L. Rosner, C. T. Sachrajda, Y. Sakai, G. P. Salam, S. Sarkar, F. Sauli, O. Schneider, K. Scholberg, D. Scott, W. G. Seligman, M. H. Shaevitz, S. R. Sharpe, M. Silari, T. Sjöstrand, P. Skands, J. G. Smith, G. F. Smoot, S. Spanier, H. Spieler, A. Stahl, T. Stanev, S. L. Stone, T. Sumiyoshi, M. J. Syphers, F. Takahashi, M. Tanabashi, J. Terning, M. Titov, N. P. Tkachenko, N. A. Törnqvist, D. Tovey, G. Valencia, K. van Bibber, G. Venanzoni, M. G. Vincter, P. Vogel, A. Vogt, W. Walkowiak, C. W. Walter, D. R. Ward, T. Watari, G. Weiglein, E. J. Weinberg, L. R. Wiencke, L. Wolfenstein, J. Womersley, C. L. Woody, R. L. Workman, A. Yamamoto, G. P. Zeller, O. V. Zenin, J. Zhang, R.-Y. Zhu, G. Harper, V. S. Lugovsky and P. Schaffner, *Phys. Rev. D: Part., Fields, Gravitation, Cosmol.*, 2012, **86**, 010001.
52 M. Ackermann, M. Ajello, A. Allafort, E. Antolini, L. Baldini, J. Ballet, G. Barbiellini, D. Bastieri, K. Bechtol, R. Bellazzini, B. Berenji, R. D. Blandford, E. D. Bloom, E. Bonamente, A. W. Borgland, E. Bottacini, T. J. Brandt, J. Bregeon, M. Brigida, P. Bruel, R. Buehler, S. Buson, G. A. Caliandro, R. A. Cameron, P. A. Caraveo, C. Cecchi, A. Chekhtman, J. Chiang, S. Ciprini, R. Claus, J. Cohen-Tanugi, J. Conrad, F. D'Ammando, A. de Angelis, F. de Palma, C. D. Dermer, E. d. C. e. Silva, P. S. Drell, A. Drlica-Wagner, T. Enoto, L. Falletti, C. Favuzzi, S. J. Fegan, E. C. Ferrara, W. B. Focke, Y. Fukazawa, Y. Fukui, P. Fusco, F. Gargano, D. Gasparrini, S. Germani, N. Giglietto, F. Giordano, M. Giroletti, T. Glanzman, G. Godfrey, S. Guiriec, D. Hadasch, Y. Hanabata, A. K. Harding, M. Hayashida, K. Hayashi, D. Horan, X. Hou, R. E. Hughes, M. S. Jackson, G. Jóhannesson, A. S. Johnson, T. Kamae, H. Katagiri, J. Kataoka, M. Kerr, J. Knödlseder, M. Kuss, J. Lande, S. Larsson, S.-H. Lee, F. Longo, F. Loparco, M. N. Lovellette, P. Lubrano, K. Makishima, M. N. Mazziotta, J. Mehault, W. Mitthumsiri, A. A. Moiseev, C. Monte, M. E. Monzani, A. Morselli, I. V. Moskalenko, S. Murgia, T. Nakamori, M. Naumann-Godo, S. Nishino, J. P. Norris, E. Nuss, M. Ohno, T. Ohsugi, A. Okumura, M. Orienti, E. Orlando, J. F. Ormes, M. Ozaki, D. Paneque, J. H. Panetta, D. Parent, V. Pelassa, M. Pesce-Rollins, M. Pierbattista, F. Piron, G. Pivato, T. A. Porter, S. Rainò, M. Razzano, A. Reimer, O. Reimer, M. Roth, H. F.-W. Sadrozinski, C. Sgrò, E. J. Siskind, G. Spandre, P. Spinelli, A. W. Strong, H. Takahashi, T. Takahashi, T. Tanaka, J. G. Thayer, J. B. Thayer, O. Tibolla, M. Tinivella, D. F. Torres, A. Tramacere, E. Troja, Y. Uchiyama, T. L. Usher, J. Vandenbroucke, V. Vasileiou, G. Vianello, V. Vitale, A. P. Waite, P. Wang, B. L. Winer, K. S. Wood, Z. Yang and S. Zimmer, *Astrophys. J.*, 2012, **756**, 4.
53 K. Lodders, *Astrophys. J.*, 2003, **591**, 1220–1247.
54 H. Benhabiles-Mezhoud, J. Kiener, V. Tatischeff and A. W. Strong, *Astrophys. J.*, 2013, **763**, 98.
55 N. Indriolo, B. D. Fields and B. J. McCall, *Astrophys. J.*, 2009, **694**, 257–267.
56 S. P. Reynolds, *Annu. Rev. Astron. Astrophys.*, 2008, **46**, 89–126.